

NO-A189 285

THE EFFECTS OF LONGITUDINAL ROUGHNESS ELEMENTS UPON THE 1/1  
TURBULENT BOUNDARY LAYER(U) UNIVERSITY OF SOUTHERN  
CALIFORNIA LOS ANGELES R F BLACKWELDER ET AL 1988

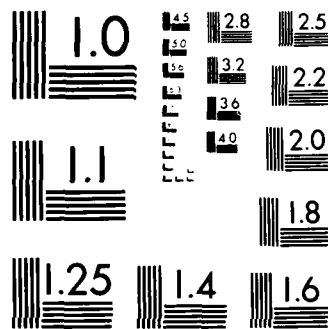
UNCLASSIFIED

N00014-86-K-0679

F/G 20/4

NL





MICROCOPY RESOLUTION TEST CHART  
NATIONAL BUREAU OF STANDARDS-1963-A

THE EFFECTS OF LONGITUDINAL ROUGHNESS ELEMENTS  
UPON THE TURBULENT BOUNDARY LAYER

R.F. Blackwelder\* and J.B. Roon\*\*  
University of Southern California  
Los Angeles, California

N00014-86-K-0679

DTIC FILE COPY

DTIC  
ELECTE  
DEC 1 1 1987

**Abstract**

Velocity profiles and bursting statistics were measured in the presence of cylindrical longitudinal roughness elements (LREs) and compared to similar work by Johansen and Smith.<sup>1</sup> An algorithm was devised to detect low speed streaks (LSS) from the hot-wire rake data, allowing an estimation of the LREs ability to reduce spatial randomness of the sublayer structure. The velocity profiles agree with Johansen and Smith's result that the effects of the LREs are felt only for  $y^+ \leq 15$ . The analysis of the bursting statistics and LSS algorithm output shows that the flow relaxes back to a flat plate boundary layer between the LREs. A crude first approximation is that the LREs simply impose the no-slip boundary condition at an elevation equivalent to their diameter. While the LREs might serve as a nucleation site for the LSS, spatial randomness of the structure is effected only very close to the LREs.  $\leftarrow$

**I. Introduction**

Turbulence production in bounded turbulent shear flows occurs primarily in the buffer layer and lower logarithmic region where  $5 < y^+ < 50$ . This domain is dominated by a sequence of events that is collectively called the "bursting process". This sequence begins with the LSS which are elongated regions of low speed fluid aligned in the streamwise direction. The LSS may be the result of streamwise vortices which removed the low speed fluid from the wall region. The LSS migrate away from the wall and portions are lifted upwards, possibly due to an instability mechanism. As these regions are ejected further outward and interact with the higher speed fluid above, a violent mixing occurs which results in considerable production of turbulent energy. This entire process occurs randomly in space and time. Hence, even though much is known about the dynamics of this process, it has been impossible to locally alter the process because the location of its occurrence was not known a priori.

Johansen and Smith introduced longitudinal roughness elements into the sublayer and concluded that the low speed streaks could be focused over these modifications.<sup>1</sup> The resulting reduction of the LSS spatial randomness would be conducive to turbulence modification schemes such as selective suction. The present investigation was embarked upon to more fully explore the reduction in spatial randomness of the sublayer structure due to the presence of the LREs.

**II. Equipment and Procedures**

The experiments were conducted in the Linac closed-return wind tunnel at USC with the LREs added to the flat plate (Figure 1) allowing parallel investigations of the normal boundary layer behavior and the case of the added LREs. The specifications of the flat plate and wind tunnel as well as a thorough discussion of the VITA technique for measuring bursting frequency are given by Blackwelder and Haritonidis.<sup>2</sup>

The boundary layer was tripped 45 cm downstream of the leading edge of the plate. The trip consisted of a strip of metal 90 cm long, 2.5 cm wide, and 0.6 cm deep. Grooves of 0.3 cm radius were placed every 1.25 cm along the strip, and the edges perpendicular to the flow were rounded to produce a three-dimensional trip. At the measurement station 5 m downstream of the leading edge, the Reynold's number based upon momentum thickness and a free stream velocity of 5 m/s was  $\approx 3400$  for all of the data taken.

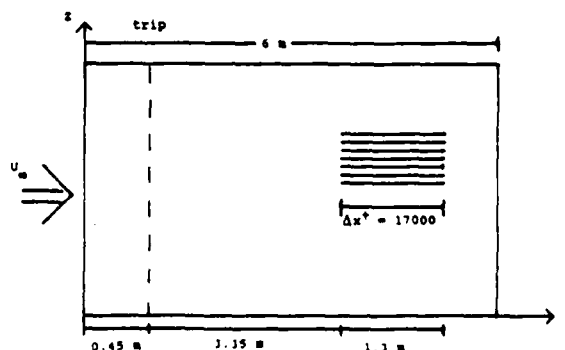


Figure 1: Modified Flat Plate with LREs.  
Spanwise spacing:  $\Delta x^+ = 80$   
LRE height :  $H^+ = 5$

\* Professor, Aerospace Engineering, Member  
\*\* Student Member

Copyright © 1988 American Institute of Aeronautics and Astronautics, Inc. No Copyright is asserted in the United States under Title 17, U.S. Code. The U.S. Government has a royalty-free license to exercise all rights under the copyright claimed herein for Governmental purposes. All other rights are reserved by the copyright owner.

**DISTRIBUTION STATEMENT A**

Approved for public release;  
Distribution Unlimited

Holes were drilled in the plate, and common fishing line was threaded through them, resulting in twelve longitudinal roughness elements. The streamwise length of each segment was 1.3 m. When scaled with the inner variables  $u_\tau$  (friction velocity) and  $\nu$  (viscosity), they had a length of  $\Delta x^+ = 17000$ . The diameter of the fishing line was chosen so that the LREs extended to a height of  $H^+ = 5$  above the plate. The spanwise spacing of the LREs was designed to coincide with the most probable spacing of the LSS ( $\Delta z^+ = 80$ ) as found by Metzler and Smith.<sup>3</sup>

A single constant temperature hot-wire was used for the velocity profiles, and a spanwise rake of eleven hot-wires was used in the bursting statistics and LSS measurements. The 1.5 cm wide rake spanned three LREs. All of the data were taken two cm upstream of the end of the LREs, and at a height corresponding to  $y^+ = 12$  above the plate. Flow visualizations using a hydrogen bubble wire in a water channel with similar LRE modifications were taken at various heights for qualitative information.

To count and measure low speed streaks, data from the hot-wire rake were analyzed in the following way. Each hot-wire measured a velocity signal as illustrated in Figure 2a.

A reference mean velocity was subtracted, and each signal was scaled with a reference rms velocity (Figure 2b). A threshold of one rms below the mean was applied (Figure 2c). When the velocity signal dropped below the threshold, the beginning of a potential low speed streak was defined. The amount of time that the signal exceeded the threshold was recorded (Figure 2d), and if this time was less than a set time (i.e., if the "length" of the potential LSS was less than some minimum "length"), the streak was rejected as an anomaly. Otherwise it was accepted as a low speed streak. Thus the following three statistics could be measured: 1) the number of streaks seen per unit time at each sensor, 2) the percentage of time that each sensor was inside a LSS, and 3) the average time of passage of an LSS over a sensor. If the LREs inhibit the spatial variation of the LSS, then the hot-wires over the strings should see significant differences in the LSS statistics as compared to the hot-wires located between the LREs and the data from a flat plate.

It should be noted that the LSS detection algorithm was very sensitive to the threshold and minimum time used in acceptance of a potential low speed streak. Variation of these parameters could produce nearly any value that the user wanted. It was not the purpose of this investigation to find the "correct" values, rather to set them in a reasonable manner and analyze the changes induced upon the statistics due to the presence of the LREs. For all of the following LSS data, the threshold was set to -1 (i.e., one rms below the mean), and the minimum time (scaled with the inner variables) was set to  $t^+ = 20$ .

Figure 2a: Velocity Signal

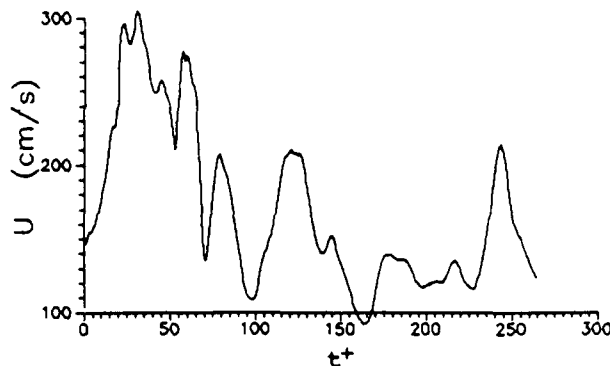


Figure 2b: Scaled Signal

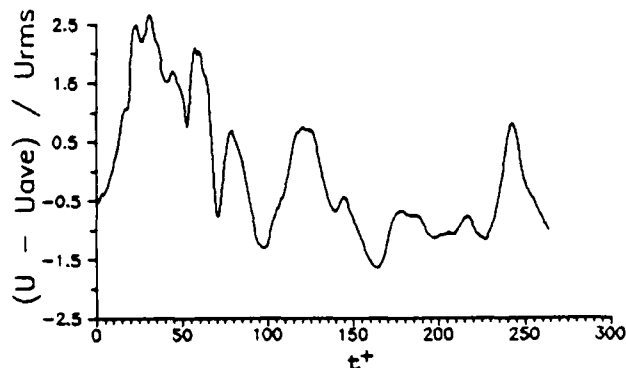


Figure 2c: Threshold at -1.0

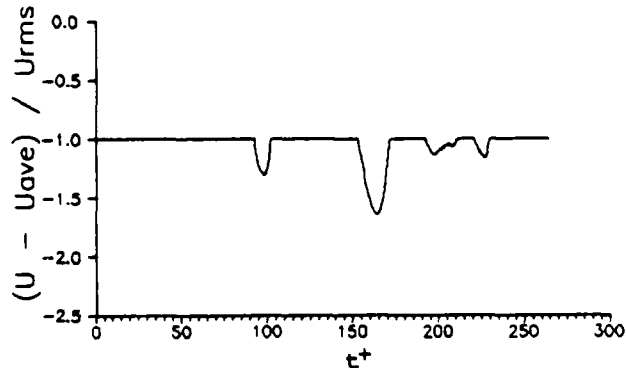
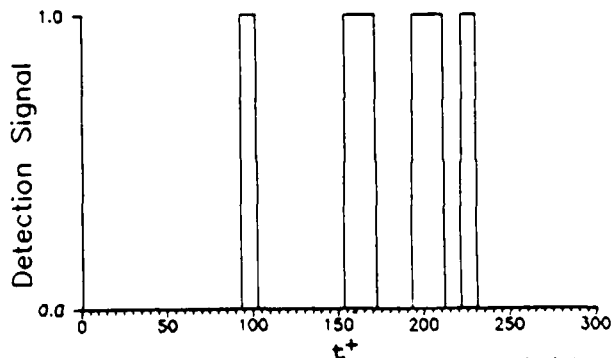


Figure 2d: Potential LSS



Availability Codes

Avail and/or  
Special

1st



A-1

A difficult question arose concerning which values to use for the reference mean and rms velocities. Both the VITA scheme for measuring bursting statistics, and the ISS algorithm presented here, hinge upon the values used. A hot-wire over a string sees a lower mean and rms velocity (Figure 3) due to the elevated no-slip condition imposed by the LRE. Two philosophies were developed to look at the data. The first was to pretend that the presence of the LREs was unknown, and use the normal flat plate values as a reference. Since the flat plate velocities are larger than those over the strings at the same height (relative to the plate), this condition triggered the ISS algorithm a greater portion of the time. The second idea was to use the local mean and rms velocities seen by each sensor, thus the various algorithms would be triggered at a lesser rate. All of the following data is presented and discussed under both viewpoints. The term "flat plate reference" refers to using the flat plate mean and rms velocities in the algorithms, and the term "local reference" refers to using the mean and rms velocities seen locally in those algorithms.

Figure 3a: Average Velocity across the span with LREs.  
( $y^+ = 12$ )

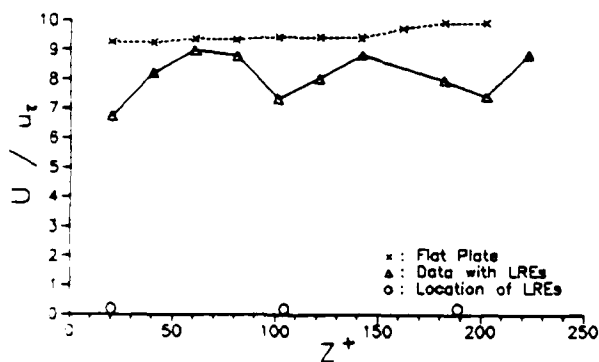
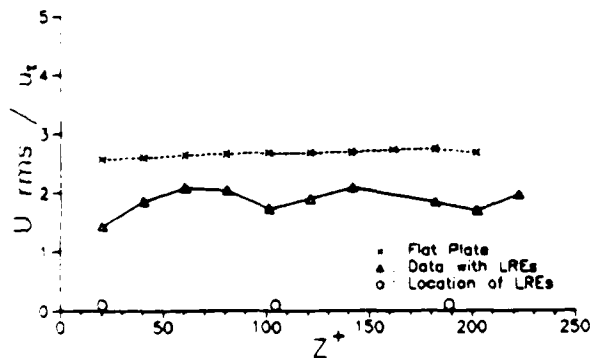


Figure 3b: Rms Velocity across the span with LREs.  
( $y^+ = 12$ )



### III. Results and Discussion

Velocity profiles directly over an LRE and between two LREs are shown in Figures 4a and 4b, respectively. The friction velocity was obtained with a Coles fit of the logarithmic region.<sup>4</sup> The friction velocities obtained in this manner were the same for all of the profiles, indicating an insensitivity of the logarithmic region to the presence of the LREs. All of the profiles are identical for  $y^+ > 15$ , thus the LREs only effect the structure of the flow in the sublayer and the buffer layer. Below  $y^+ = 15$ , there is a velocity deficit over a string, and an excess between them, as would be expected. It should be noted, however, that if the data over an LRE is shifted by the diameter of that LRE ( $H^+ = 5$ ), the defect disappears and a normal boundary layer profile is obtained. Hence velocity profiles over an LRE appear to be simply elevated by the height of that LRE.

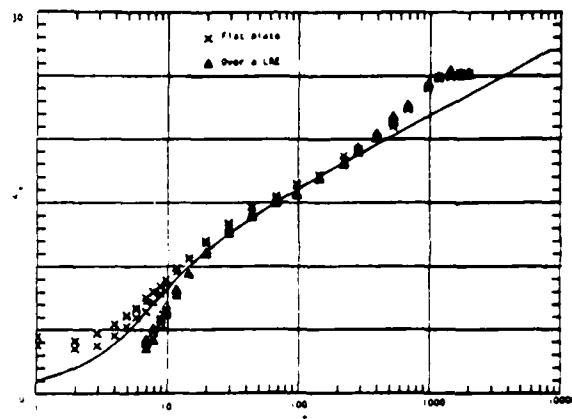


Figure 4a: Velocity Profiles over an LRE. The multiple data points are for different runs and indicate the repeatability of the data.

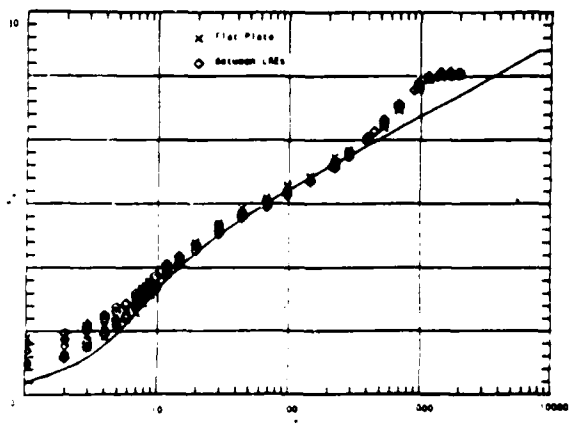


Figure 4b: Velocity Profiles between LREs. The multiple data points are for different runs and indicate the repeatability of the data.

Figure 5a is a hydrogen bubble visualization at a height of  $y^+ = 6$  relative to the plate. The flow is from top to bottom in the picture. There are indications of LSS over all but one of the strings, and a few streaks are discernable between them. First appearances would suggest that the LSS have a great affinity for the LREs. Figure 5b is a similar visualization at a height of  $y^+ = 12$ . Although the average spacing of the LSS is comparable to the spacing of the LREs by design, the actual location of the LSS is quite random with respect to the LREs. However, it may be possible to associate most of the streaks as "belonging" to one or another of the strings. A sketch of iso-velocity contours over the LREs (Figure 5c) reveals that the no-slip condition imposed by an LRE requires that relatively low speed fluid will surround the LRE. The right side of the sketch demonstrates that if the LSS were forced over corresponding LREs, the spanwise velocity fluctuations would move the streaks randomly perpendicular to the LREs. This dislocation would increase with elevation, and hence the LSS would appear randomly with respect to the LRE. Thus, above a certain height, it would be impossible to determine which streak originated at which LRE. The data presented here would place that height at  $y^+ = 10$  to 15.



Figure 5a: Hydrogen Bubble Visualization with the LREs ( $y^+ = 6$ ).



Figure 5b: Hydrogen Bubble Visualization with the LREs ( $y^+ = 12$ ).

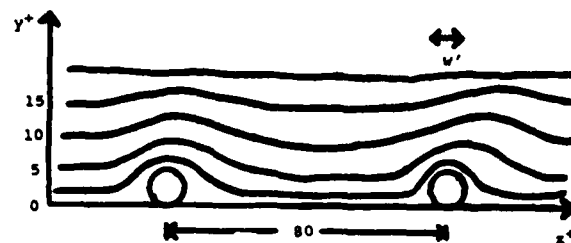


Figure 5c: Sketch of Instantaneous Iso-velocity Contours Over LREs.

All of the data plotted in figures 6, 7, 8, and 9 were taken at a height of  $y^+ = 12$  relative to the plate. The data from a normal boundary layer on a clean plate at the same height are also plotted. The rake could not be operated below this height because heat conduction directly to the strings biased the results. If the only effect of the LREs was to elevate a normal boundary layer by their diameter, then the statistics over an LRE (when referenced locally) should compare to the flat plate values at a height of  $y^+ = 7$ . The extra dashed lines in figures 6b, 7b, 8b, and 9b represent such flat plate information obtained with a single hot-wire.

In figure 6a, the bursting frequency for the LREs and a clean plate are shown. These data were calculated with the flat plate reference velocity values. The bursting frequency approaches zero over a string, while the values between the strings are comparable to the flat plate values. In Figure 6b, the local reference values were used in the VITA algorithm, and peaks in the bursting frequency are seen above the strings. This is expected since the VITA algorithm calculates its own mean value based upon a short temporal average, consequently it is independent of the mean velocity value. Thus the number of bursts detected is inversely proportional to the applied rms threshold. Since the LREs reduce the rms values, one expects a larger number of burst detected. This is seen in Figure 6b as compared to 6a. An important indication that the LREs do not fully eliminate the randomness of the LSS is indicated by the bursting frequency between the LREs which has the same magnitude as the flat plate value. The graphs show that

Figure 6a: Bursting Frequency across the span. (flat plate reference,  $y^+ = 12$ )

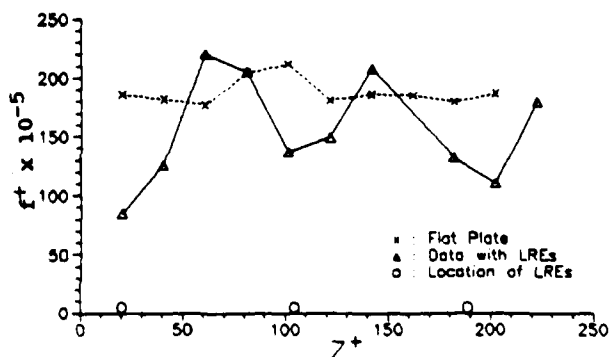
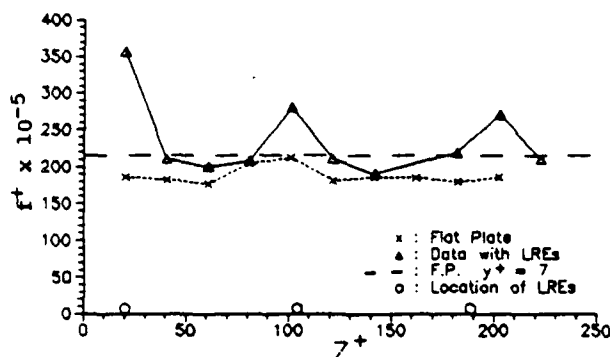


Figure 6b: Bursting Frequency across the span.  
(local reference,  $y^+ = 12$ )



while the streaks may "prefer" bursting over an LRE, there is no reduction of bursting between the LREs. Thus the spatial randomness of the entire bursting process is only effected near the LREs.

The number of LSS seen per second, based on the flat plate reference, are plotted in Figure 7a. The frequency of the detected LSS appears to have doubled over the LREs, but is not significantly reduced between them. At first glance, it would seem that the LREs are generating their own LSS in addition to those already existing in a normal boundary layer. But as discussed earlier (Figure 5c), the elevated no-slip condition creates lower velocities over the strings. Thus when referenced to the flat

Figure 7a: Number of LSS seen per second across span.  
(flat plate reference,  $y^+ = 12$ )

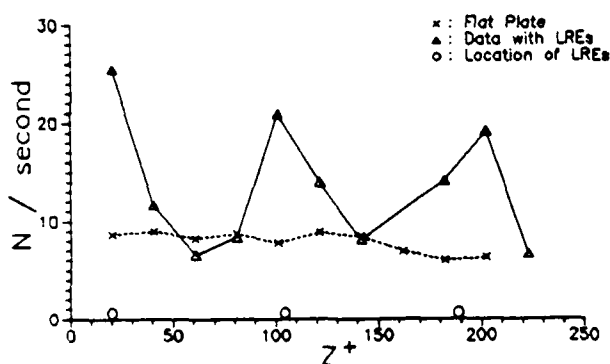
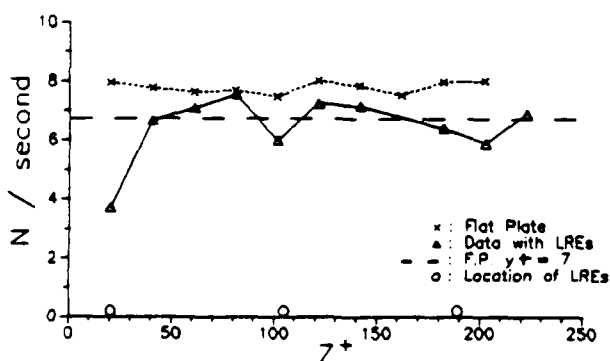


Figure 7b: Number of LSS seen per second across span.  
(local reference,  $y^+ = 12$ )



plate, the LSS algorithm is triggered more often. Using the local reference, Figure 7b shows a lower number of streaks seen per second over the LREs. Again, the values between the LREs are comparable to the flat plate data.

Figures 8a (flat plate reference) and 8b (local reference) represent the percentage of time a hot-wire is inside of a LSS during the data run. The LREs impose a lower velocity, hence generate the appearance of additional low speed streaks when referenced to the flat plate (i.e., the flat plate reference is equivalent to increasing the threshold in Figure 2c above -1). Between the strings, a sensor spends the same percentage of time in a LSS as a sensor over a clean plate. For the local reference conditions, the velocity fluctuations over an LRE exceed the threshold less frequently. Correspondingly Figure 8b shows a smaller percentage of time spent inside an LSS for the sensors directly over LREs.

Figure 8a: % of Time in a LSS across the span.  
(flat plate reference,  $y^+ = 12$ )

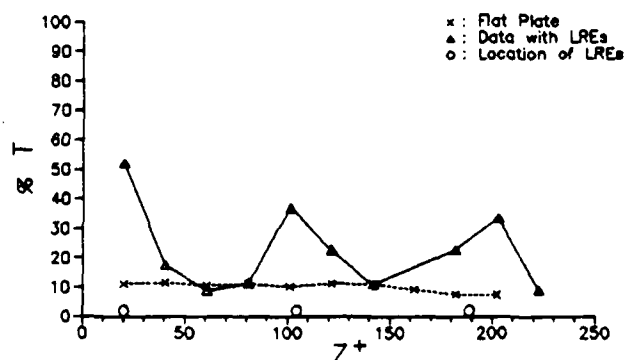
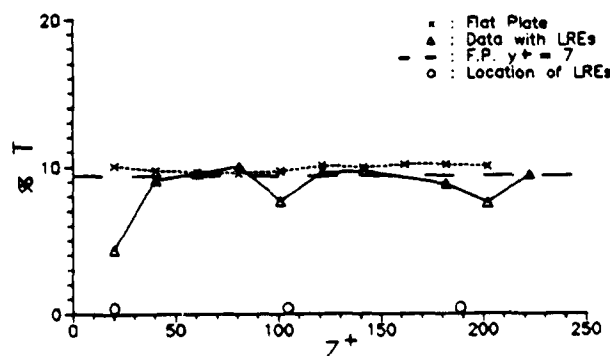


Figure 8b: % of Time in a LSS across the span.  
(local reference,  $y^+ = 12$ )



Figures 9a and 9b show the average time of passage of an LSS over the sensors. This information could be converted into the average lengths of the LSS using Taylor's hypothesis, but the appropriate value of the convection velocity is unclear. The same trends due to the elevated no-slip condition are seen over the LREs. And again the values between the LREs are comparable with the clean flat plate values. A low speed

streak is in general orientated at some small angle with respect to the free stream direction. If the LSS really locked onto the LREs, then this angle should decrease, and the streaks seen by the hot-wires would appear "longer". In Figure 9b, all of the data lie within the scatter, and no lengthening trend is apparent.

The dashed line in figures 6b, 7b, 8b, and 9b that represents flat plate data for  $y^+ = 7$  usually appears closer to the values over the LREs than any of the other data points. The exception is Figure 9b where the scatter prohibits any conclusions. Thus a crude first approximation would be to say that the LREs simply elevate the no-slip condition locally, and could be modeled by the normal flat plate statistics being raised by the diameter of the LREs.

Data were also obtained at other values of  $y^+$ . At  $y^+ = 18$  the data show a complete relaxation back to a clean flat plate, and the LREs are "invisible" to the sensors above them. Any tendency for an LSS to be aligned with a particular LRE is apparently destroyed by the spanwise velocity fluctuations by the time the LSS extends out to this altitude.

Figure 9a: Average Time of Passage of a LSS across the span.  
(flat plate reference,  $y^+ = 12$ )

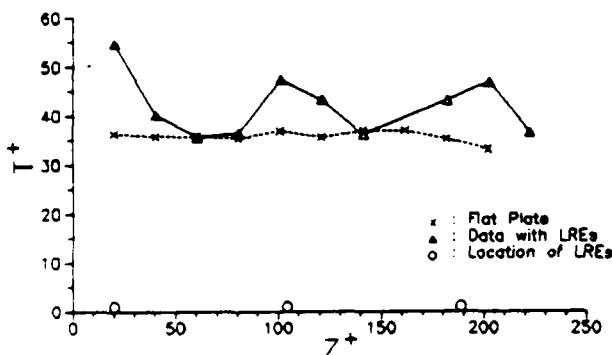
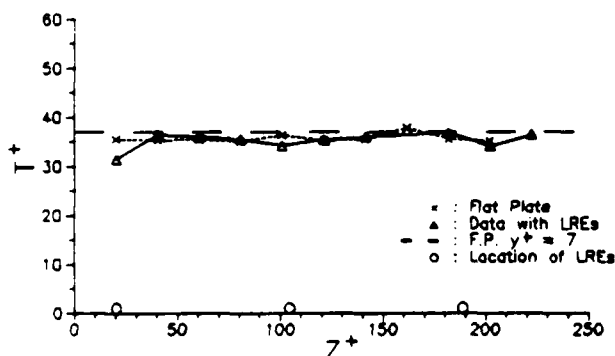


Figure 9b: Average Time of Passage of a LSS across the span.  
(local reference,  $y^+ = 12$ )



#### IV. Conclusions

The visualization results of Johansen and Smith<sup>1</sup> and the present work indicate that the LSS are focussed over the LREs for  $y^+ \leq 10$ . However the velocity measurements presented in figures 3 and 4 indicate that this result is due to the no-slip boundary condition over the LREs, and consequently one expects to see a lower velocity near the LREs.

The mean velocity profiles indicate that the average low speed fluid above the LREs extends outward to  $y^+ \approx 20$ , whereas the regions between the LREs showed very little effect on the mean profile. The role of the spanwise velocity seems to be important in randomizing the LSS. That is, even though the LSS are associated with the LREs at  $y^+ = H^+$ , the lower speed fluid above the LRE is buffeted in the spanwise direction at slightly higher elevations as illustrated on the right hand side of Figure 5c. The data at  $y^+ = 18$  (not shown) suggest that this process is so strong that the LSS appear to be completely random for  $y^+ \geq 15$ .

The bursting frequency and low speed streaks detected across the span show a trend of relaxation back to flat plate boundary layer values between the strings. If the LSS were perfectly aligned over the LREs, then the bursting frequency and the number of streaks should tend to zero between the LREs. Since the data measured between the LREs is comparable with the flat plate values, the spatial randomness of the sublayer structure is only decreased in a region very close to the roughness elements.

One of the remaining questions is whether the small amount of order imposed by the LREs is sufficient to assist in turbulent modification schemes. If the turbulence modification depends only upon the structure at the wall, the LREs may impose sufficient order to be of assistance. However if the modification depends upon the structure being locked in space above  $y^+ \approx 15$ , it is doubtful that LREs will be useful.

#### V. Acknowledgements

This research was supported by the National Aeronautics and Space Administration under Contracts NAS1-17951 and NAS1-18292 and the Office of Naval Research under the University Research Initiative Contract N00014-86-K-0679.

The authors wish to extend special thanks to Mr. Frank Pray and to Mr. Scott Hutcherson for obtaining the hydrogen bubble visualizations used herein.

#### VI. References

1. Johansen, J.B. and Smith, C.R., 1986, "The Effects of Cylindrical Surface Modifications on Turbulent Boundary Layers", *AIAA Journal*, 24, 1081.
2. Blackwelder, R.F. and Haritonidis, J.H., 1982, "Scaling of the Bursting Frequency in Turbulent Boundary Layers", *J. Fluid Mech.*, 122, 87.
3. Smith, C.R. and Metzler, S.P., 1983, "The Characteristics of Low-Speed Streaks in Near-Wall Region of a Turbulent Boundary Layer", *J. Fluid Mech.*, 122, 27.
4. Coles, D.E., 1968, "The Young Person's Guide to the Data", *Proceeding of the Computations of Turbulent Boundary Layers - 1968, AFOSR-IFP-Stanford Conference*, 2, Mechanical Engineering, Stanford, CA.



END

DATE

3-88

DTIC